Alternating PSM balancing characterization: A comparative study using AIMS and wafer print data

Martin Sczyrba[1], Roderick Köhle[2], Karsten Bubke[1], Mario Hennig[3], Rainer Pforr[3], Ralf Neubauer[1]

[1]Advanced Mask Technology Center GmbH & Co. KG, Raehnitzer Allee 9, D-01109 Dresden, Germany;
[2]Memory Products, Infineon Technologies AG, Germany;
[3]Infineon Technologies SC300 GmbH & Co.KG, Germany

ABSTRACT

Alternating Phase-Shifting masks (altPSM) are known to provide high contrast imaging combined with a low Mask Error Enhancement Factor (MEEF) at low k1. At feature sizes close to 60nm half-pitch and less the impact of mask topography effects increases. This applies in particular for altPSM. This is due to the quartz etch which is required for every second mask aperture to obtain the 180 degrees phase shift. It enlarges the mask profile height significantly. The influence of the quartz trench profile on the transmission and phase balancing performance has already been studied extensively. Basically it has been shown, that tighter quartz trench profile control, specifically for etch depth and width, is required with decreasing mask feature half pitch.

The desired mask pattern geometry optimization is currently based on an evaluation of the printed resist pattern over defocus. However, a mask process engineer can use instead only AIMS measurements of the mask features. Therefore there is a mature interest to check, how good such measurements can replace resist pattern measurements.

In the paper therefore it is evaluated how accurate AIMS measurements can describe the real printing performance of an alternating PSM in resist. Impact of differences of the image formation is investigated by use of analytical expressions. Furthermore, the influence of tool imperfections and the presence of resist are discussed. The theoretical results are compared to experimental data taken from AIMS measurements and wafer prints.

Keywords: Alternating phase-shifting mask, Phase Balancing, AIMS, Resist Model

1. INTRODUCTION

Alternating Phase-Shifting masks (altPSM) are one common approach to provide excellent imaging performance for low k_1 applications [1]. This is achieved by imposing a 180 degrees phase shift on the light transmitted through every second mask opening. The desired phase shift can be gained by etching into the quartz at those openings. Doing so requires a high accuracy in achieving this etch depth with a reasonable accuracy and uniformity over the entire mask. Also, due to scattering of the light in these openings there might be a difference in the transmission of neighboring openings. This effect is usually taken into account already at design level. Here a biasing of the width of quartz etched and non-quartz etched mask apertures is applied. In addition an under-etch can be applied. In this case the quartz is not only etched vertically to gain the phase shift but also horizontally below the chromium. The quality of these correction methodologies can be quantified by measuring the clear CDs formed by two neighboring openings. A mask is called balanced if the difference of these CDs vanishes for all focus settings. In other words, if a difference in the clear CDs is observed through-focus, the mask suffers from imbalancing. The amount of imbalancing and its lithographic impact can be determined from the function $\Delta CD(z)$, which describes the clear CD difference as function of defocus z, [2], [3].

This function is determined differently in a wafer fab or a maskshop. A wafer fab determines it from either wafer prints or from measuring the width of the trenches after etching. These are the actual lithographically relevant values. In contrast a maskshop usually does not have the opportunity to obtain these data. As an alternative the Aerial Image Measurement System (AIMS) can be utilized to gain insight in the printing behavior of the mask. For this purpose the mask is illuminated with settings similar to those used at the scanner. The formed image is collected by a CCD sensor. From the intensity distribution obtained this way the function $\Delta CD(z)$ can be determined. However, there are some obvious differences in the way the imbalancing is measured. To get information on the quality of a mask or to derive an optimal correction scheme, one needs to make sure, that wafer prints and AIMS measurements can be well correlated.

Once a correlation like this is established some interesting options arise for the wafer fab as well as the maskshop. On one side, a mask can be specified directly by its printing behavior via AIMS measurements instead of currently common indirect measurements, like e.g. etch depth. On the other side, an engineer in the maskshop can tailor the mask making processes best to the customer needs based on AIMS measurements.
For these reasons there is an interest in investigating the differences in the imaging of the two tool types and their impact on the measured imbalancing of the mask. The paper is organized as follows: firstly we describe the systematic differences in the determination of imbalancing based on wafer prints and AIMS measurements. The differences concerning the image formation and their impact are described and quantified in the following sub-section. Discussed after that, is the impact of the resist on the correlation. In a following section we illustrate the analytically derived results by experimental results.

2. SYSTEMATIC DIFFERENCES IN PHASE BALANCING MEASUREMENTS AT AIMS AND STEPPER

As briefly outlined above there are several systematic differences in the processes of determining altPSM imbalancing done by utilizing AIMS measurements compared to the actual results obtained by printing the mask in a wafer fab. These differences fall mainly into two classes: the creation of the intensity distribution by the imaging system and the "measurement" of it. This "measurement" at an AIMS tool is done by a direct measurement of the intensity using a CCD sensor. On the other hand, the intensity created by the stepper is "measured" by the developed resist. For these two ways of determining the intensity distribution there is no straightforward way of establishing a correlation other than directly comparing the measurement results. Even under the (not valid) assumption, that the image by the AIMS and the Stepper optics were the same and it is correctly measured by the CCD sensor, the existence of the resist and its processing can lead to highly non-trivial deviations between the CDs measured in resist and those determined from the intensity. In order to correctly derive their correlation one needs a model for the resist and its processing which is absolutely accurate and not based upon measurements of mask prints. Such a model is not available. Furthermore, the correct relation between the developed resist profiles and the CD measured by, for example, a CD-SEM would be required. In section 3*e* we discuss in more detail the impact of resist profiles and their modeling for altPSM.
A first step towards including the resist and its processing is to use a threshold model. For this purpose the image created by stepper at the surface of the resist (air or an immersion liquid) needs to be calculated. Then the impact of Fresnel loss at the incoupling of the intensity at the resist/surface interface, the propagation of the waves through the resist to the desired depth and the contributions from waves reflected back from the underlying wafer stack need to be considered. In this paper we will simplify this task by considering the intensity in resist just below the resist/surface interface and assuming the resist to be infinitely thick to avoid the back-reflection from the wafer stack.
On the other hand already the imaging process in the optics of an AIMS tool shows several differences to those by the scanner. These differences are due to the different concepts underlying the two tools. The AIMS tool is a microscope which magnifies the image created by some part of the mask, whereas the scanner demagnifies the image created by the entire mask. The two tools are constructed such, that the diffraction pattern created by mask is equally limited at the object side of the projection optics, thus, the object-side NAs are identical. The image-side NAs, on the other hand, are not equal to achieve a magnification for one tool but a demagnification for the other tool. The image-side NA of an AIMS tool is very small, which means that the propagation of the emitted waves can be considered as paraxial. For a scanner the image-side NA is large and, therefore, the waves here can be emitted under large angles. This requires a vectorial treatment of these waves, whereas for an AIMS tool the waves can be treated in scalar approximation. Also, the impact of defocusing is different in the two cases. We derive analytical expressions for the image of a mask formed under these different conditions below and compare the impact of these effects on the imbalancing measured in the intensity distribution.
In addition to the differences described so far, there are tool imperfections, which can be different from tool to tool. To name just a few, there are flare, aberrations, source imperfections and tool stability issues. We discuss the impact on the imbalancing measurement for some of them in section 3*c* and 3*d*.

3. IMAGING OF ALTERNATING PHASE-SHIFTING MASKS

The intensity distribution given by illuminating an altPSM containing a dense lines and spaces pattern is created by interference of 3 diffraction orders. The 1st and the -1st orders create the desired image of the array and the, only for a

not balanced mask existing, 0th order adds an additional sinusoidal with a period twice as large as the period of the array. Use of incoherent illumination is not changing this but only leads to a reduction of the contrast of the image. The principal way of image formation and a typical image is shown in Fig. 1.
In this section we will use an analytical expression, which relates the intensity distribution to properties of a Kirchhoff mask to derive an analytical expression for the difference in neighboring clear CDs. This will be done for coherent illumination. An extension to partially coherent illumination with perfect and imperfect sources is done by the use of simulations.

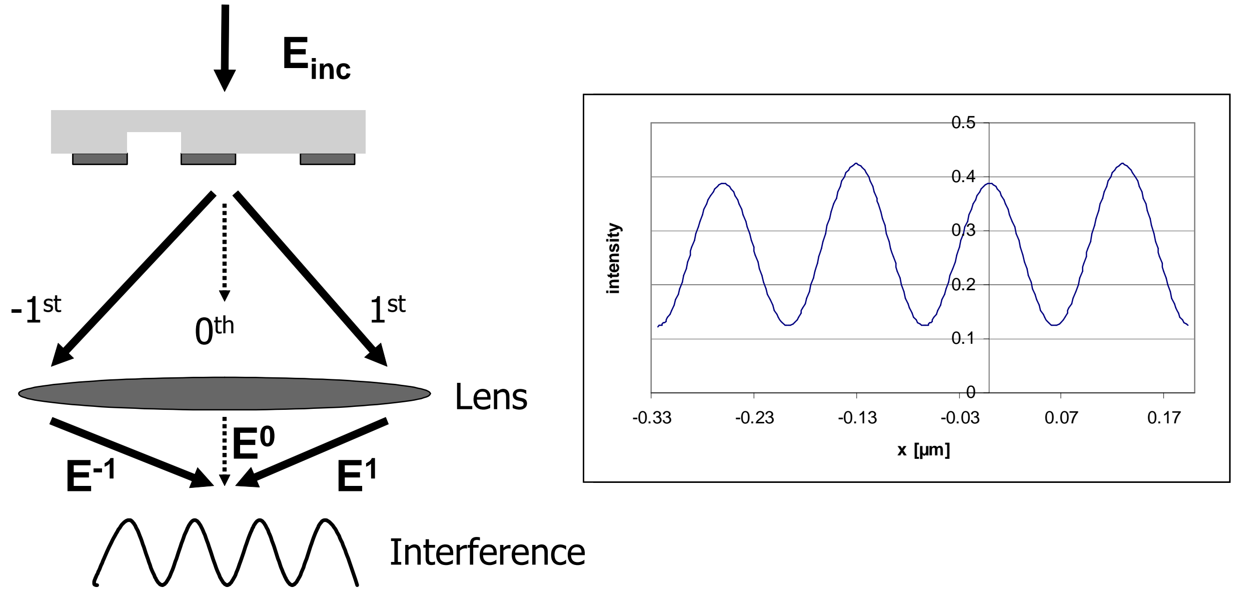

Figure 1: Image formation (left) and typical image (right) of an imbalanced altPSM.

a) Imaging with coherent light
The image formed by 3-beam interference of -1st, 0th and 1st diffraction order can generally be written as:

$$I(x,z) = \beta_0 + \beta_1(z)\cos\left(\frac{2\pi}{p}x + \alpha\right) + \beta_2\cos\left(\frac{4\pi}{p}x\right), \tag{1}$$

where p is the pitch of the array creating the image. Also, z denotes the distance of the image plane to the focal plane. The parameters β_i depend on the duty cycle, the phase and the transmission of the mask. Especially, if the mask is balanced β_1 vanishes. Furthermore, α equals zero if there is no difference in phase and absolute value of the 1st and the -1st diffraction order.
As described previously, an imbalancing of the mask leads to differences in the clear CD of neighboring intensity maxima. This can be explained by the additional modulation given by the second term in equation (1). The difference mainly depends on the defocus and on the intensity threshold chosen for the evaluation.
For a balanced mask the clear CD is identical to the half-pitch of the array for an intensity threshold equal to the averaged intensity, β_0. If this threshold is chosen, one can approximate the difference of neighboring clear CDs as:

$$\Delta CD(z) \approx -\frac{p}{\sqrt{2}\pi}\frac{\beta_1(z)}{\beta_2}. \tag{2}$$

As can be seen this expression vanishes for all focus settings if β_1 is zero, thus, the mask is balanced. A similar expression has been derived in [4].

The detailed form the expression depends on form of the β_i, which themselves depend also on the way the intensity distribution is created by the imaging system. As has been discussed previously, there are systematic differences in the image formation by a scanner compared to an AIMS tool. These differences result in different expressions for the β_i. For the calculations of prefactors we considered imaging in scalar approximation for the AIMS tool, which leads to:

$$\beta_0 = 2\left|E^1\right|^2 + \left|E^0\right|^2, \tag{3}$$

$$\beta_1(z) = 4\left|E^1\right|\left|E^0\right|\cos\left[\frac{2\pi}{\lambda}\left(1-\sqrt{1-\frac{\lambda^2}{p^2}}\right)z + \Delta\phi_{10}\right], \tag{4}$$

and:

$$\beta_2 = 2\left|E^1\right|^2, \tag{5}$$

where E^0, E^1 are the amplitudes of the 0th and 1st diffraction orders and $\Delta\phi_{10}$ is the phase difference between these order.

For image formation in a scanner the electric field representing the diffraction orders needs to be treated as a vector and different polarization states have to be considered. Doing so one gets:

$$\beta_0 = 2\left|E^1\right| + \left|E^0\right|, \tag{6}$$

$$\beta_1(z) = 4\left|E^1\right|\left|E^0\right|[1+\cos\alpha]\cos\left[\frac{2\pi}{\lambda}\left(1-\sqrt{1-\frac{\lambda^2}{p^2}}\right)z + \Delta\phi_{10}\right], \tag{7}$$

and:

$$\beta_2 = 2\left|E^1\right|^2\left[1+\cos^2\alpha - \sin^2\alpha\right], \tag{8}$$

where α is given by pitch:

$$\sin\alpha = \frac{\lambda}{p}. \tag{9}$$

In both cases the assumption was made that the 1st and -1st diffraction orders have identical amplitudes and phases. Also no mask polarization effects were considered here. So, the amplitudes of the orders in TE and TM polarization state were considered being equal. Furthermore, the incoupling into the resist in the case of the scanner has not been considered so far.

Under both imaging conditions the defocus dependence of the CD difference is given by a cosine function whose period is determined by ratio of the illumination wavelength and the pitch of the imaging array. At a constant wavelength this period decreases with the array pitch. In Fig. 2 CD differences obtained from AIMS measurements are shown. Each curve corresponds to an array of dense lines and spaces at a given pitch. One finds that over a fixed range of defocus the function $\Delta CD(z)$ tends more to a cosine-like behavior as the pitch is decreased.

For the focus region, which usually is of interest it, thus, may has been sufficient to consider $\Delta CD(z)$ as a linear function. From this approach the imbalancing of an altPSM can be specified by the offset and slope [5], defined as:

$$offset = \Delta CD(z=0) \tag{10}$$

and

$$slope = \left.\frac{d\Delta CD}{dz}\right|_{z=0}. \tag{11}$$

This may no longer be sufficient for smaller pitches where the focus region covers a large part of the cosine's period. Then an extrapolation of the CD difference by using offset and slope over the entire focus range leads to an overestimation of it. Also, offset and slope have a stronger dependence on the determination of best focus. For example,

in Fig. 2 the slope for the array with pitch of 360nm is constant. This is no longer the case for smaller pitches where a shift in best focus will lead to a different slope. This is important to notice as in cases like these the description by offset and slope is not sufficient and higher derivatives might be necessary to consider. Alternatively, the amplitude of the cosine function or simply the maximal CD deviation over the focus range of interest can be investigated.

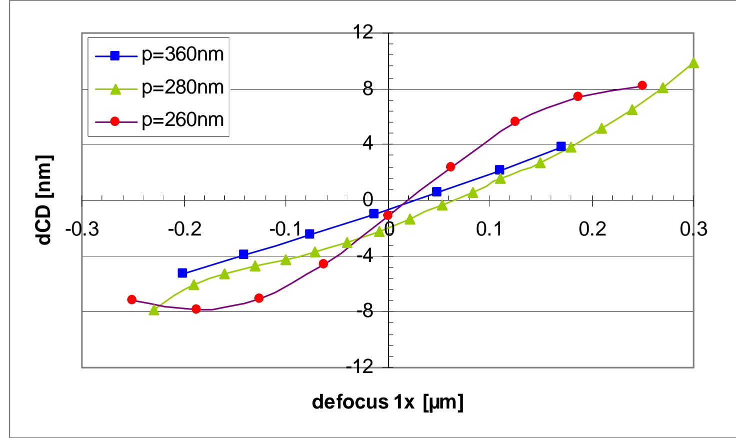

Figure 2: Differences in neighboring CDs of arrays with different pitches measured using the AIMS tool.

Before we study in detail the correlation between imbalancing measured at the AIMS tool and at the scanner, two other systematic differences in imaging will be discussed. These are the obliquity factor and the coupling of the intensity into the resist. To correctly take into account energy conservation in the imaging systems the obliquity factor needs to be considered [6]. This factor weighs diffraction orders differently according to the angle under which it is emitted by the mask. In the present case of altPSM imaging only the first diffract orders are affected. As can be seen in Fig. 3 the obliquity factor for the AIMS tool is almost equal to one for all pitches, whereas for the scanner it increases with pitch. This results in an increase of the amplitude of the first diffraction order. As the imbalancing is given by the ratio of the amplitudes of 0th to the 1st diffraction order this decreases the measured imbalancing.
Another difference in the image creation is the medium in which the image is formed. For an AIMS tool this is air whereas for a scanner the image is formed in resist. Despite the fact the actually resist profiles are used to determine the imbalancing which depend on several parameters, like wafer stack, resist processing, exposure etc., we will here limit ourselves to the intensity distribution. If this is considered in resist one has to include the incoupling of the diffraction orders into resist and maybe even the propagation into the resist film. For sake of simplicity, we here focus on the first aspect. For that purpose we define: the intensity distribution is always measured directly under the resist surface. There we also define the focal plane of the imaging system to be. Also we assume that the resist film is infinitely thick, thus, no energy is reflected back from the underlying stack. Under these assumptions, the impact of the resist is given by the Fresnel loss at the surface/resist interface. This loss is a damping of the amplitudes of the diffraction orders, depending on its angle of incidence and its polarization state.Details on these damping factors can be found in [6].
As is shown in Fig. 3, the main impacts of the Fresnel loss on the measured imbalancing is due to the larger damping of the 1st diffraction orders compared to the 0th order. As the ratio between zero and first order increases, the imbalancing is also increased. Also the Fresnel losses damp the TE component stronger than the TM component which increases the vector effects.
Incorporating these two effects into the formulae above one can now derive an expression for the correlation of the imbalancing measured in the intensity distribution created by an AIMS tool compared to one created by a scanner and projected into the resist:

$$\Delta CD_{Scanner}(z) = C_{\Delta CD} \cdot \Delta CD_{AIMS}(z) \tag{12}$$

where:

$$C_{\Delta CD} = \frac{O_{AIMS}}{O_{Scanner}} \frac{T_0 \left[T_1^{TE} + T_1^{TM} \cos(\alpha)\right]}{\left(T_1^{TE}\right)^2 + \left[\cos^2(\alpha) - \sin^2(\alpha)\right]\left(T_1^{TM}\right)^2} . \tag{13}$$

Here the factors T_0, T_1^{TE} and T_1^{TM} are the damping factors for the Fresnel loss of the respective diffraction order and polarization state. Again, this expression was derived under the assumption that no mask polarization effects are present.

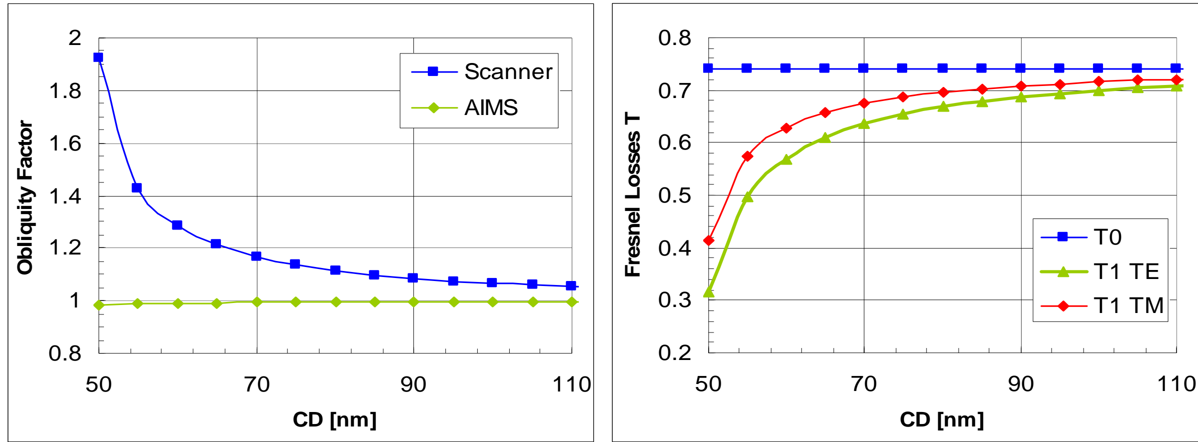

Figure 3: Oliquity factors (left) and strength of Fresnel loss (right) for different diffraction orders and polarization states for various pitches.

This result shows that effects considered so far only change the amplitude of the function $\Delta CD(z)$. Nevertheless, offset and slope are, of course, also impacted. For the offset the correlation factor between AIMS and scanner imaging is identical to $C_{\Delta CD}$. It is shown in Fig. 4 for various combinations of effects, which were incorporated. It can be seen that some effects increase the imbalancing measured at the stepper compared to AIMS, like for example, vector effects and Fresnel loss, whereas other effects, like the obliquity factor, decrease the imbalancing. As all of these effects depend on the angle under which light propagates through the optics or leaves it, the correlation factor depends on the pitch of array considered. In total the imbalancing measured at scanner level will be larger than those measured with the AIMS as the pitch gets smaller and smaller. However, one has to bear in mind that for smaller pitches the impact of polarization increases which has not been considered here. For the pitches investigated here the impact of mask polarization can be neglected.

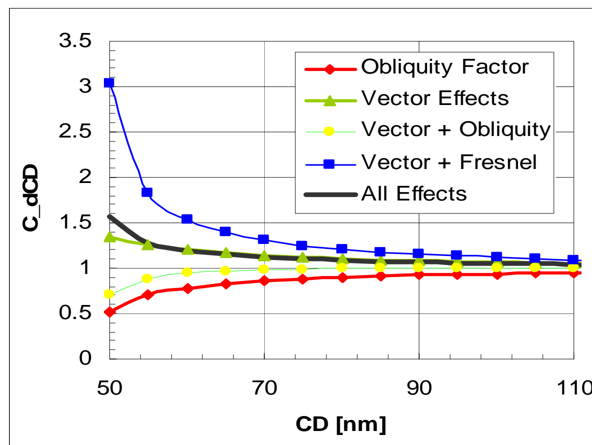

Figure 4: Correlation factor for amplitude of $\Delta CD(z)$ and offset for various pitches. Also shown is the impact of single effects on the correlation factor.

A similar picture unveils for the relation of the slopes. The correlation factor is given by:

$$slope(scanner) = \frac{2p^2}{\lambda^2}\left[1-\sqrt{1-\frac{\lambda^2}{p^2}}\right]\cdot C_{\Delta CD}\cdot slope(AIMS)\,. \tag{14}$$

It has a similar form as the correlation factor for the offset but with an additional prefactor. This is due to the derivative with respect to defocus. The net impact of vector effects, obliquity factor and Fresnel loss on the correlation of the slope can be seen in Fig. 5.

To conclude, the systematic differences in the way the image of an altPSM is created in a stepper and in an AIMS tool leads to differences in the imbalancing determined in the two systems. The correlation factors for the maximal CD difference, offset and slope are close to one for arrays with pitches above 180nm but increase significantly for smaller pitches.

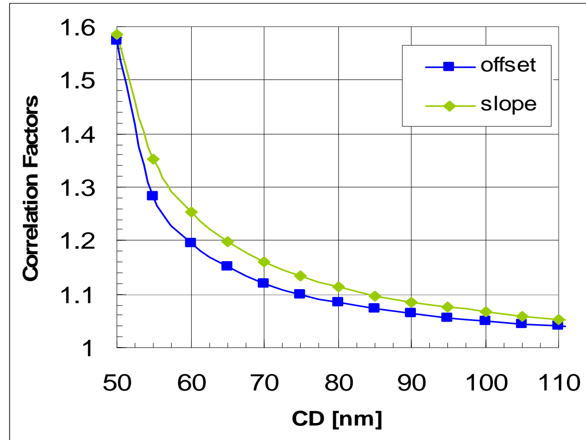

Figure 5: Correlation factors for offset and slope for various pitches.

b) Imaging with partially coherent Light

The calculations presented so far assumed that the imaging is done with coherent light. For practical applications this assumption is never satisfied and question arises of how the results change as the incoherence of the illumination is increased. This will be investigated in this section.

From a physics point of view the partially coherent illumination leads to an incoherent addition of intensity distributions formed by coherent light which is entering the mask under certain angles. These angles range from zero (coherent illumination) to a maximum angle given by the coherence (σ) and the NA of the imaging system. In principle, one can perform similar calculations as described above for an arbitrary angle of incidence on the mask and integrate over all angles to obtain the final image. Doing so leads to an integral expression for which no closed form can be found. An alternative is the description of the image by transmission cross coefficients which can be computed for fixed illumination settings [6]. An approximate solution for imaging of altPSM with partially coherent light can found in [4]. We here use simulation results to illustrate the major effects.

In Fig. 6 offset and slope as function of partial coherence are shown for a Kirchhoff mask with pitch=130nm and transmission of 0.95 and phase of 175° in the phase-shifting area. On the left side (a) the mask was illuminated with scanner conditions and the image projected into an infinitely thick resist with n=1.7. The result for illumination with AIMS conditions and projection into air is shown on the right side (b). The imaging was done using NA=0.85.

One can see that in both cases the measured imbalancing is increasing with increasing σ used. This is due a reduction of the contrast which is different for the two sinusoidal involved. The contrast loss is stronger for the sinusoidal representing the actual array image which leads to an effective increase of the measured imbalancing. This effect depends on the ratio of σ and NA. It can be seen that the imbalancing stays constant at an value calculated for coherent imaging until a certain level of incoherence is reached and then increase drastically. This effect is due to the limiting NA. For coherent imaging the diffraction orders can be seen as monopoles located within the circle determined by the

image-side NA. As the incoherence of the illumination increases these monopoles become circles with increasing radii. For some value of σ the circles representing the first diffraction orders hit the rim of the pupil and, if σ is increased further, some light from these orders can not pass the NA of the system.
The contrast of the array image is determined by the interference of the first diffraction orders, which both are affected by the cut-out at the rim. The sinusoidal determining the imbalancing is given by the first and the zero-th order, where the later is not affected. This explains the difference in contrast loss for both sinusoidal and the resulting increase of measured imbalancing for increased incoherence.

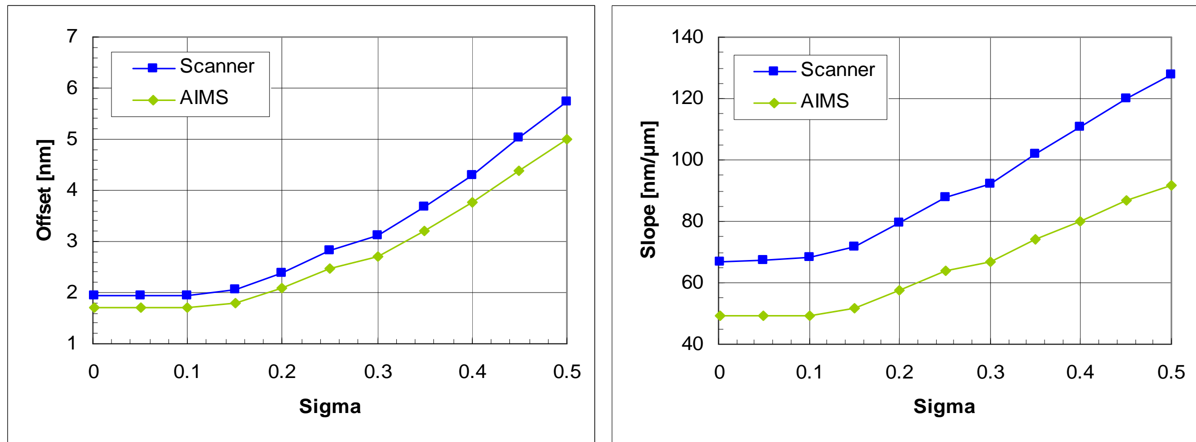

Figure 6: Offset (left) and slope (right) as function of partial incoherence.

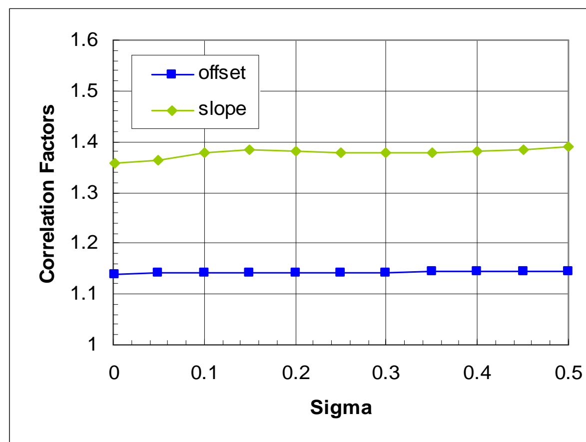

Figure 7: Correlation factors for offset and slope measured at scanner and AIMS vs incoherence of illumination.

Despite the discussed increase of absolute values of offset and slope for increasing incoherence in illumination the correlation factors between scanner and AIMS illumination remains almost unchanged. This is illustrated in Fig. 7.
Thus, the correlation derived for coherent imaging can still be used.

c) Impact of Abberations

After having discussed systematic deviations in the imaging by the two different exposure tools, a second class of differences will be considered now. The results so far were derived assuming an ideal imaging process. This assumption is also not valid for practical applications. We will, thus, investigate the impact of two prominent tool imperfection, lens aberrations and source inhomogeneity.

It is a well-known fact that every exposure tool operating with high numerical apertures suffers from the impact of lens aberrations. The effect caused by them is a deformation of the wave fronts leaving the optical system. This deformation leads to different positions of the points, which the waves finally converge to. The deformation usually depends on the position at which the wave leaves the projection lens. The impact on the diffraction by deformed wave fronts can be described by changes of the phase of the waves, usually expressed in terms of Zernike polynomials. For the purpose of this study we will use aberrations which change the relative phase between 0th and first diffraction orders or between the first diffraction orders themselves. Two representative examples for such Zernikes are Z5 and Z7, also called astigmatism and coma. The astigmatism Z5 changes the phase of the -1st and 1st identically while leaving the 0th order unchanged. As can be seen from equation (2) the phase difference between these orders acts like a phase-shift on the function $\Delta CD(z)$. Therefore, one expects the maximum CD difference to be unchanged but offset and slope to vary due to a shift of the cosine function. This indeed can be seen in Fig. 8 where the simulated CD difference vs defocus is shown for various strengths of Z5 for AIMS illumination settings with NA=0.85 and σ=0.33. The mask considered was again a Kirchhoff mask with pitch=130nm, phase=175°, transmission=0.95 for phase-shifting areas.

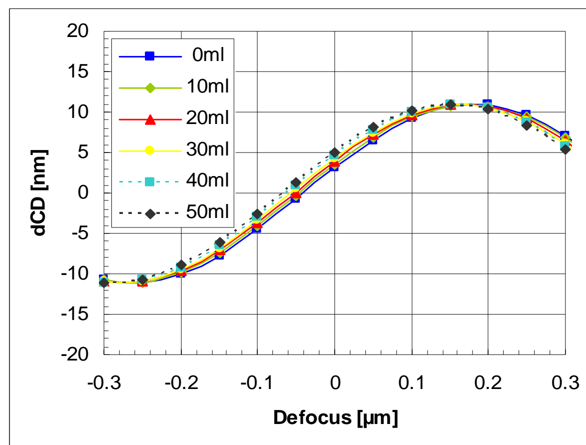

Figure 8: Impact of aberration Z5 on the CD difference for various defocus settings (AIMS tool).

The offsets and slopes determined from each curve are shown in Fig. 9. It can be seen that significant changes can be found in the presence of this type of aberration.

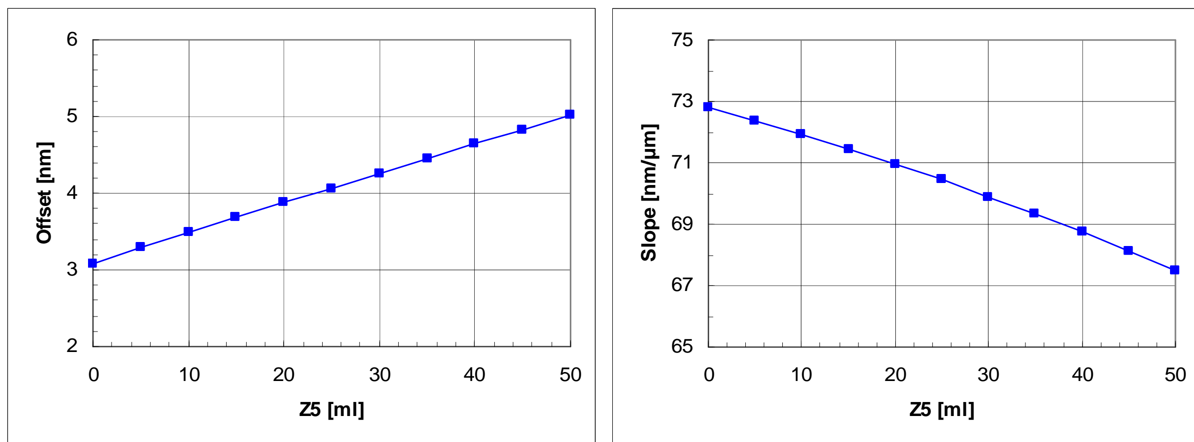

Figure 9: Impact of aberration Z5 on the offset and slope (AIMS tool).

As discussed, Z5 mainly acts as a focus shift for the CD differences. Whether this impact has a practical relevance strongly depends on the way of how best focus is determined. For example, if the best focus is determined via a contrast optimization and Z5 is the only tool imperfection, than this impact is not visible.
The other type of aberration, Z7, now changes the phases of -1st and 1st diffraction orders in a way that one diffraction order experiences an increase in phase whereas the phase of the other is reduced by the same amount. The 0th order again remains unchanged. The interpretation of the impact of these changes goes beyond the validity of equation (2) as it was derived under the assumption that the phase of -1st and 1st diffraction order is identical. From the theory one obtains, that a difference in the phases of these two orders results in a phase shift of the two sinodials in this equation. The amount of the shift is proportional to the difference in phase. The shift of the sinodials prevents from an easy interpretation of the resulting difference in CDs. Simulation under the same conditions as for the other aberration type were performed. One finds that this type of aberration has almost no impact on the measured imbalancing.
To conclude, it has been shown that aberrations can have a strong influence on the measured imbalancing, especially as typically the strength of aberrations are different for a scanner compared to an AIMS tool. To quantify their impact is difficult, depending not only on the type of aberration but also on details of the exposure process. In particular the way of how the best focus is determined is of high importance.

d) Impact of Source Intensity Inhomogeneity

Another type of tool imperfection which has an impact on the measured imbalancing is the intensity homogeneity of the illumination source. It has been shown previously that strong inhomogeneity of the source can falsify the measurements done with an AIMS tool [7]. As for the aberrations the source homogeneity is also of importance because it will be different for a stepper compared to an AIMS or even between two different scanners or AIMS tools.
Here an example will be used to illustrate the impact of the source imperfection. The same mask as for the aberrations was illuminated with a perfect source and with a measured intensity distribution from an AIMS tool with same nominal illumination settings of NA=0.85 and a small σ. The resulting CD differences are shown in Fig. 10. The values for offset and slope determined for these cases can be found in Tab. 1.

	Perfect Source	Real Source
Offset [nm]	3.1	2.8
Slope [nm/μm]	72.8	68.6

Tabelle 1: Offset and Slope for imaging with a perfect source and a real source (AIMS).

One finds that in this example the imbalancing measured decreases for the real source. This will not be true in general as the detailed impact of the source imperfection strongly depends on its characteristics. Nevertheless, this is an aspect which needs to be considered for any attempt to correlate scanner with AIMS measurement results.

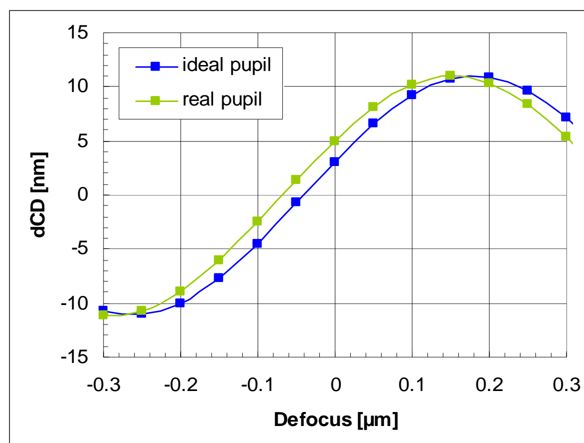

Figure 10: Differences in CD vs defocus simulated using a perfect source and a real source with NA=0.85 and small σ.

e) Impact of Resist

Beside the differences in the image formation as discussed so far there is another fundamental difference between the way imbalancing is measured by wafer prints and by using an AIMS tool. This is the presence of the resist. It is the developed resist image which is measured in a wafer fab to judge the printing performance of a mask. Unfortunately there is no trivial correlation between the intensity distribution projected into the resist film by the scanner and the developed resist profiles. This is due to the complex processes which interact during the resist exposure and the following development phase.
These processes and their interactions can hardly by described in simple analytical models. For that reason numerical models have been established that take them into account. In order to use them input needs to be feed into the models to determine their parameters. The accuracy and extendibility of the models predictions strongly depend on this input. For the purpose of the present study this approach is actually not valid as we want to describe the impact of the resist. If we measure this impact and feed it into the model we can only extrapolate this input without guaranteeing the accuracy. One would actually need a resist processing model that is based on first principles. Due to the complexity of the process such a model is not available. Thus, one can only use the approach described above.
However, any calibrated resist model needs to be set up based on data representing imbalanced masks structures as well as balanced structures. This is to ensure the predictability of the model for the case of imaging of imbalanced masks. Currently an investigation is on going to determine the impact of the resist by the use of such a model.

4. EXPERIMENTAL RESULTS

For an experimental verification of the simulation results presented above an altPSM was manufactured at the Advanced Mask Technology Center Dresden. The mask was balanced using a combined dry and wet quartz etch process. The mask design consists of dense lines and spaces with various pitches, chrom widths and biases of the openings. Furthermore, the depth of the quartz etch was varied to study the impact of imbalancing. This mask has been extensively measured at the AIMS tool and also wafer prints at Infineon Dresden were done at the same locations as of the AIMS measurements. At each measurement the differences in the clear CDs for various focus settings was determined.

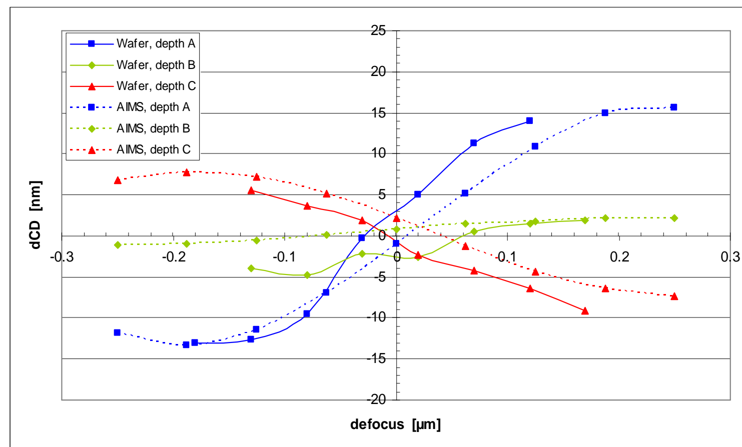

Figure 11: Differences in neighboring clear CDs vs defocus at three different etch depths measured at AIMS and determined from wafer prints.

In Fig. 11 the CD differences at three different etch depths are shown determined from AIMS measurements and from wafer prints. One finds, that the qualitative behavior shows good agreement but quantitatively differences appear. These differences can be explained by the systematic differences described above and also by the impact of the resist processing.
One problem in the experimental verification is that, first of all the scanner image can only be examined by the resulting resist image and also, obviously not all sources for differences can be varied, e.g. strength of aberrations. One therefore always has to compare the resulting net effect. However, as one example were the a single effect can be shown the

coherence of the illumination at the AIMS tool was varied to show its impact on the imbalancing. For that purpose one structure of the altPSM was illuminated with an increasing incoherence of the circular aperture at constant NA=0.85. As predicted above, this leads to an increase of the measured imbalancing which can be seen in Fig. 12.

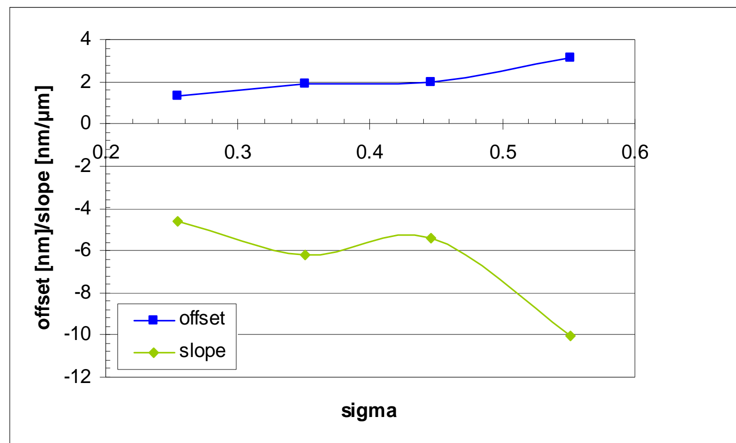

Figure 12: AIMS-measured imbalancing of an altPSM vs partial coherence of the illumination.

As described above an altPSM with varying balancing quality was made to study the correlation between AIMS-measured imbalancing and the results of wafer prints at the similar position on the mask. The results are shown in Fig. 13 were the offset and slope determined from the wafer prints and those measured with the AIMS tool are plotted against each other. For the pitch of 130nm used for the experiment, theory predicts correlation factors of ~1.14 for the offset and ~1.4 for the slope. The experimentally measured factors are summarized in Tab. 2.

Scanner/AIMS	Experiment	Theory (w/o resist processing)
Offset	0.68	1.14
Slope	1.33	1.4

Tabelle 2: Comparison of correlation factors for offset and slope determined from experiments and theory.

One finds that the measured correlation factors are lower than those predicted from theory. However one has to bear in mind that the predicted factors do not include effects due to the resist processing. The experimental data seem to indicate that this impact tends to equalize the measured values. As discussed in sub-section *e* of the last section the impact of the resist is only very little understood so far. Future investigations need to work closer on that subject to establish this missing link.
Also one has to consider that offset and slope strongly depend on the determination of best focus. There are differences in the way this is done for wafer prints and for AIMS measurements. In order to determine best focus in a wafer fab usually a focus-exposure matrix is recorded. From this the isofocal point on the CD versus focus curve at the dose-to-size is obtained and treated as best focus. In contrast, the best focus for an AIMS measurement is given by the focus setting that yields maximum contrast of the image. A study on what the difference in best focus values from these definitions is a study is ongoing. To illustrate the possible impact, the best focus in the AIMS measurements was artificially changed and the correlation factor to the unchanged wafer results was determined. The focus shift was realized by fitting a cosine function to the experimtally determined CD differences. Using this function offset and slope were determine at various focus positions. The results are shown in Fig. 14. One finds that a variation of 50nm in best focus can change the factors by 10% and more. Thus, the definition of best focus is another crucial point to understand the correlation of AIMS and wafer measured phase balancing.

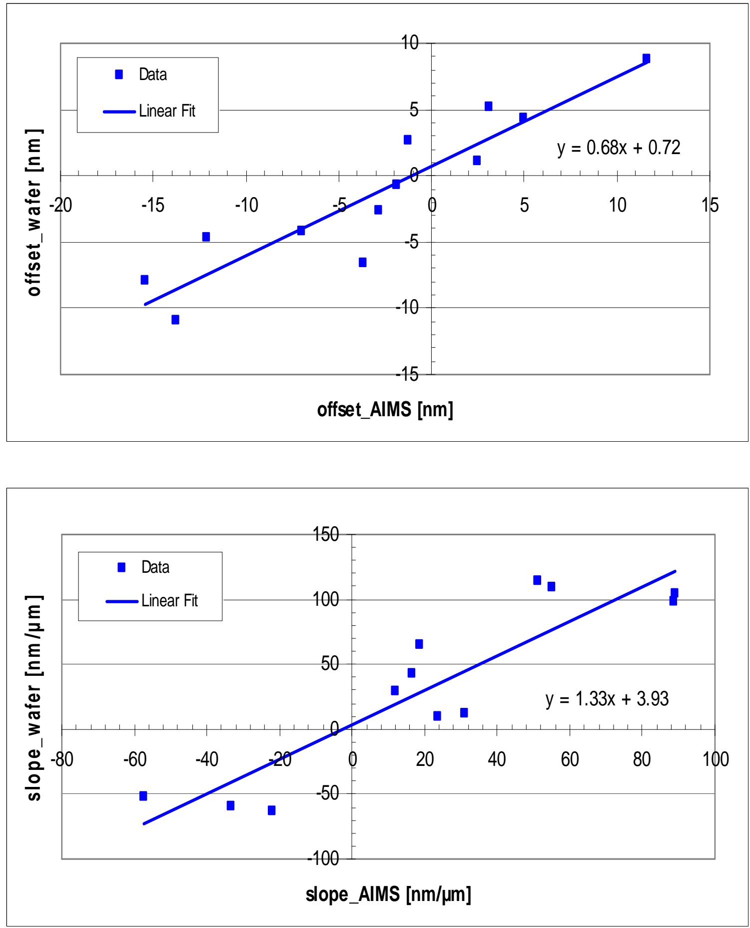

Figure 13: Correlation between offset (top) / slope (bottom) determined from wafer prints and AIMS measurements.

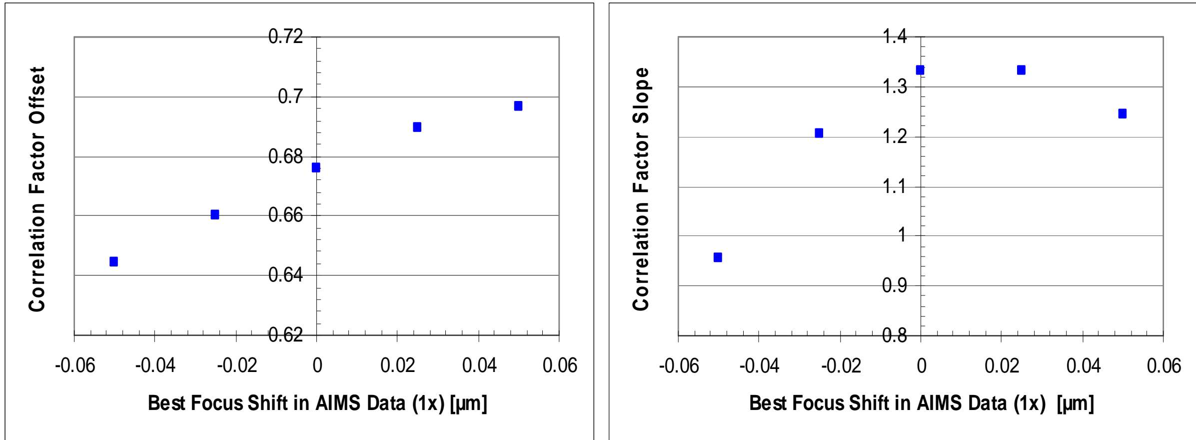

Figure 14: Correlation factor between Scanner and AIMS for offset (left) and slope (right) for various settings of best focus in the AIMS measurements.

Another important effect that has not been taken into account is flare. It has been shown that flare has an impact on the measured phase balancing [8]. As it is very likely that the flare level is different for a scanner compared to an AIMS tool flare can have an impact on the correlation too.

5. CONCLUSIONS

In this paper we investigated the systematic differences in the imaging of altPSM between a scanner and an AIMS tool. Expressions were derived which describe the image formation in an AIMS tool and the image created by a scanner in an infinitely thick resist stack. These expressions were used to describe the differences of the clear CDs as the defocus is varied. To measure this CD variation one can use metrics as offset/slope or maximum CD difference. For them we derived correlation factors between scanner and AIMS imaging. An experimental verification of these factors showed that only the differences in imaging cannot fully describe the correlation. Two other important factors are the resist and its processing and also the definition of best focus. The impact of these two could not be quantified in the present work. Further investigations are ongoing. However, there are more differences which were not discussed, for example flare.
Another important aspect discussed here is the dependency of the slope on the definition of best focus. It has been shown that for pitches less than 360nm the slope can change strongly if best focus is varied. Thus, potential focus offsets between AIMS measurements and wafer prints need to be considered.
The authors consider the present study as a first step towards a systematic understanding of phase balancing measurements done in a wafer fab or a mask shop. Topics were identified on which the authors suggest future studies should focus on.

ACKNOWLEDGEMENTS

This reasearch was supported by the German Federal Ministry of Education and Research (BMBF) under contract No. 01M3154A ("Abbildungsmethodiken für nanoelektrische Bauelemente").

REFERENCES

1. R. Pforr, M. Hennig, R. Koehle, N. Morgana, J. Thiele, J. Weckesser, „Hard phase-shifting masks for the 65nm node – A performance comparison", Proc. SPIE, Vol. 5377, p.212-221, 2004
2. U. A. Griesinger, L. Mader, A. Semmler, W. Dettmann, C. Noelscher, R. Pforr, "Balancing of alternating phase-shifting masks for pratical application: modeling and experimental verification", Proc. SPIE, Vol. 4186, p. 372-383, 2001
3. A. Semmler, L. Mader, A. Elner, R. Koehle, U. Griesinger, C. Noelscher, „Application of 3D EMF Simulation for Development and Optimization of Alternating Phase Shifting Masks", Proc. SPIE, Vol. 4346, p.356-367, 2001
4. S. Peng, "Through-Focus Image Balancing of Alternating Phase Shifting Masks", Proc. SPIE, Vol. 3873, 1999
5. C.E. Tabery, C.A. Spence, "Evaluation of 3D Alternating PSM structures using Mask Topography Simulation and AIMS at λ=193nm", Proc. SPIE, Vol. 4346, p.429-440, 2001
6. A. K. Wong, "Resolution Enhancement Techniques in Optical Lithography", SPIE Press, 2001.
7. A.C.Duerr, K. Bubke, M. Sczyrba, S. Angonin, "The importance of being homogenous – on the influence of illumination inhomogeneity on AIMS images", Proc. SPIE, Vol. 5992, p.859-872, 2005
8. S. Teuber, I. Higashikawa, J.-P. Urbach, C.M. Schilz, R. Koehle, A.M. Zibold, "First results from AIMS beta tool for 157nm lithography", Proc. SPIE Vol. 5377, 2004